Astron. Astrophys. 338, 75–84 (1998)

ASTRONOMY AND ASTROPHYSICS

The effect of diffusion and mass loss on the helium abundance in hot white dwarfs and subdwarfs

K. Unglaub and I. Bues

Dr. Remeis-Sternwarte Bamberg, Astronomisches Institut der Universität Erlangen-Nürnberg, Sternwartstraße 7, D-96049 Bamberg, Germany

Received 6 January 1998 / Accepted 15 June 1998

Abstract. Previous diffusion calculations failed to explain quantitatively the presence of helium in hot hydrogen rich white dwarfs and subdwarfs. We present the results of improved diffusion calculations in the range $40000\mathrm{K} \leq \mathrm{T_{eff}} \leq 100000\mathrm{K}$, $6.0 \leq \log g \leq 8.0$ with a more sophisticated treatment of the momentum transfer from photons to matter and the inclusion of ionization- and flux-blocking effects. However, the effect of all these improvements turns out to be small in comparison to the possible effect of mass loss on the surface composition, which may, compared to the results of the diffusion calculations, lead to large over- or underabundances of helium. For $T_{\mathrm{eff}} = 80000\mathrm{K}$, $\log g = 7.0$ and zero mass loss the surface helium abundance decreases from the solar one to about $\mathrm{He/H} = 10^{-3}$ within a few thousands of years, whereas in the presence of mass loss with $\dot{M} \approx 10^{-13} M_*/\mathrm{y}$ helium sinks in time scales similar to cooling ages. In contrast, mass loss rates of $\dot{M} < 10^{-14} M_*/\mathrm{y}$ lead to a strong depletion of helium. Therefore mass loss is a possible explanation for the presence of helium in DAO white dwarfs as well as for the absence of helium in DA's. Depending on the number fraction of hydrogen hidden in hot helium rich white dwarfs, a weak wind may prevent or considerably retard the floating up of hydrogen.

Key words: diffusion – stars: abundances – stars: evolution – white dwarfs – subdwarfs

1. Introduction

White dwarfs are separated in two distinct spectroscopic sequences, a hydrogen- rich and a helium-rich one. The hydrogen white dwarfs can be subdivided into two classes, the DA stars with no spectroscopically detectable helium and the DAO stars, in the spectra of which helium lines are visible. For hot DA's helium abundances have sometimes been derived under the assumption that this element provided most of the EUV opacity. However, Vennes (1992) and Koester (1989) have shown that the EUV flux deficiencies typical for DA's with $T_{\mathrm{eff}} > 40000\mathrm{K}$ can be explained either with the presence of heavy elements or by stratified H/He atmospheres. The presence of helium in the DAO's, which are with $T_{\mathrm{eff}} > 60000\mathrm{K}$ hotter than most of the DA's, is still unexplained. Vennes et al. (1988) have shown that the observed helium abundances, which are typically $10^{-3} \leq \mathrm{He/H} \leq 0.1$, cannot be explained by radiative levitation. The predicted abundances are too low by at least a factor of ten. Fontaine & Wesemael (1987) suggested that most white dwarfs enter the cooling sequence as helium-rich objects with some traces of hydrogen. In the course of time gravitational settling causes hydrogen to float up. This led to the hypothesis of thin hydrogen layers (Vennes & Fontaine, 1992), according to which the DAO's have stratified atmospheres characterized by an equilibrium between gravitational settling and ordinary diffusion. This scenario requires ultrathin hydrogen layers with masses smaller than $10^{-13} M_*$. However, Napiwotzki & Schönberner (1993) and Bergeron et al. (1994) concluded from an analysis of helium line profiles, that the atmospheres of most DAO's are more likely chemically homogeneous rather than stratified. Mass loss has been invoked as a possible explanation. The question "thick or thin hydrogen layers in white dwarfs" is rediscussed in Fontaine & Wesemael (1997) and Shipman (1997).

A similar problem occurs in hot subdwarfs with $25000\mathrm{K} \leq \mathrm{T_{eff}} \leq 40000\mathrm{K}$ and $5 \leq \log g \leq 6$ (for a review see Heber, 1992 and Saffer & Liebert, 1995). They may be subdivided into the intermediate helium-deficient sdOB stars ($\mathrm{He/H} = 0.03$ would be a typical value) which are preferably near the hot end of the T_{eff} range and the helium-poor sdB's. Michaud et al. (1989) have shown that at least in the case of sdOB's the observed abundances of helium cannot be levitated by radiative forces.

In a previous paper (Unglaub & Bues, 1996, Paper I) we have shown that the effect of the chemical composition on the temperature structure may be of importance for the predicted surface composition. Therefore in addition to hydrogen and helium the elements C, N and O are taken into account. The abundances of all these elements are predicted simultaneously. As this is an improvement of the work Vennes et al. (1988), we decided to do new diffusion calculations for white dwarfs and subdwarfs with $40000\mathrm{K} \leq \mathrm{T_{eff}} \leq 100000\mathrm{K}$ and $6.0 \leq \log g \leq 8.0$. For the elements hydrogen and helium the calculation of the radiative forces described in Paper I has been improved and ionization effects are taken into account (see Sect. 2). The diffusion calculations are time dependent with a numerical method similar to

Send offprint requests to: K. Unglaub

the one of in Unglaub & Bues (1997; Paper II). $T_{\rm eff}$ and $\log g$ remain constant during the calculations. As in Paper II a plane-parallel stratification is assumed. In Sect. 4 the influence of mass loss on the surface composition will be investigated.

2. Improvements on the diffusion calculations

For the elements hydrogen and helium ionization effects are taken into account. This momentum transfer by collisions originates from the different diffusion velocities of the hydrogen and helium particles in the various ionization states. Our method is similar to the one described by Michaud et al. (1979) and used by Vennes et al. (1988). However, it allows to account for non-zero diffusion velocities not only for helium, but for the neutral and ionized particles of the hydrogen background plasma in addition. Babel & Michaud (1991) have shown that ambipolar diffusion of hydrogen could be one of the major processes affecting the chemical abundances supported in the atmospheres of Ap stars. If thermal diffusion is neglected, from the equations of Geiss & Bürgi (1986) and Burgers (1969)

$$\frac{dp_s}{dz} - n_s m_s g + n_s Z_s e E + n_s F_{s,\rm rad} = \sum_t \left(K_{s,t} + n_t m_s \gamma_{t,s}\right)\left(w_t - w_s\right) \quad (1)$$

can be derived, where w_t and w_s are the z components of the diffusion velocities of the particle species t and s.

The resistance coefficients $K_{s,t}$ for the interaction between charged particles are obtained from Paquette et al. (1986). The most important mechanism of interaction between H and H^+ for the plasma conditions considered here is resonant charge exchange (RCE), the interaction due to polarization will be neglected. For the RCE momentum transfer cross section (see e.g. Eq. 15.4 of Suchy, 1984) of the ground state of hydrogen a constant value of $6*10^{-19}{\rm m}^2$ has been adopted, which neglects the approximately logarithmic dependence on the relative velocity of the colliding particles. According to the results of Newman et al. (1982) and Hunter & Kuriyan (1977) this is a typical value for the plasma conditions important in our work. For the excited states a scaling factor $2n^2 - 1$ proposed by Peterson & Theys (1981) has been used. The other charged and neutral particles mainly interact via polarization. With polarizabilities from Radzig & Smirnov (1985) and a polarization potential proportional to r^{-4} (Michaud et al., 1978), the collision integrals have been evaluated according to Eq. 10.31,7 of Chapman & Cowling (1970). For the interaction between the neutral atoms H and He a hard sphere approximation has been used.

$\gamma_{t,s}$ is the transformation rate of particle species t into s by ionization or recombination processes. To obtain the rates for particles in a certain ionization state, mean values over all excitation states are used, e.g. the ionization rate of hydrogen is:

$$\gamma_{\rm H,H^+} = \sum_{i=1}^{i_{\max}} \frac{n_{\rm H,i}}{n_{\rm H}} \left(C_{i\kappa} + R_{i\kappa}\right) \quad (2)$$

$C_{i\kappa}$ and $R_{i\kappa}$ are the collisional and radiative ionization rate (see Eqs. 5-79 and Eqs. 5-40 of Mihalas (1978) or Appendix C of Gonzales et al. (1995)) The number $i_{\max}$ of bound states is obtained from the Debye screening formalism and a cutoff procedure as described in Paper I. The recombination rates are obtained from detailed balancing arguments.

For each of the elements C, N and O one momentum equation, averaged over all ionization states , is used. As one of them is redundant, the one for protons is replaced by the condition of zero mass flow. These equations and the equation of radiative transfer (diffusion approximation) are solved just as described in Paper II.

An important improvement concerns the momentum transferred from photons to matter by photoionization processes. In Papers I and II has been assumed that all the photon momentum is transferred to the heavy particle. However, as the photoelectrons are preferentially ejected in forward direction, part of the momentum is given to the photoelectron. For hydrogen-like particles, this effect has been evaluated in detail by Massacrier (1996). The fraction $f_{\rm ion}^{\rm nl}$ is given for the various excitation states. So we obtain for the momentum $n_k F_{k,\rm rad,C}$ per unit volume and unit time transferred by photoionization processes to the particles in ionization state k:

$$n_k F_{k,\rm rad,C} = n_{k-1}\frac{1}{c}\int_{\nu=0}^{\infty} F_\nu \sigma_\nu^{(k-1)} f_{{\rm ion}(\nu)} d\nu - n_k \frac{1}{c}\int_{\nu=0}^{\infty} F_\nu \sigma_\nu^{(k)} \exp\left(-\frac{h\nu}{kT}\right) d\nu \quad (3)$$

The factor $\sigma_\nu^{(k-1)} f_{{\rm ion}(\nu)}$ represents the monochromatic absorption cross section per particle in ionization state $k-1$ corrected by the factor $f_{\rm ion}$. It is a weighted mean value over the various excitation states. The first expression on the right hand side of the equation above represents the momentum transferred on the particles in ionization state k by photoionizations of particles in ionization state k-1. The residual photon momentum is given to the free electrons. The second term accounts for the recoil on the particles in ionization state k which is due to photorecombination processes of particles in ionization state $k+1$. It has been derived from an emission rate obtained from detailed balancing arguments and the boson factor, which predicts, that photons are preferably emitted in direction of the radiation flux (for details see e.g. Oxenius, 1986). For neutral helium the values of $f_{\rm ion}$ for the hydrogenic case have been used. According to Massacrier & El-Murr (1996) they do not differ very much from the exact values.

In the corresponding Eq (25) of Paper I for $F_{k,\rm rad,C}$ is a misprint, the right hand side of which must be multiplied with a factor n_{k-1}/n_k. (The results of Paper I are not affected, however, because the corresponding equation in the computational code has been correct).

In contrast to Paper I, the line profiles for the lines of He^+ and H have been evaluated in detail with the data from Underhill & Waddell (1959) and a probability distribution function for the electric microfield at a charged point from Hooper (1967). In the computation of the radiative force on He^+ due to bound-bound

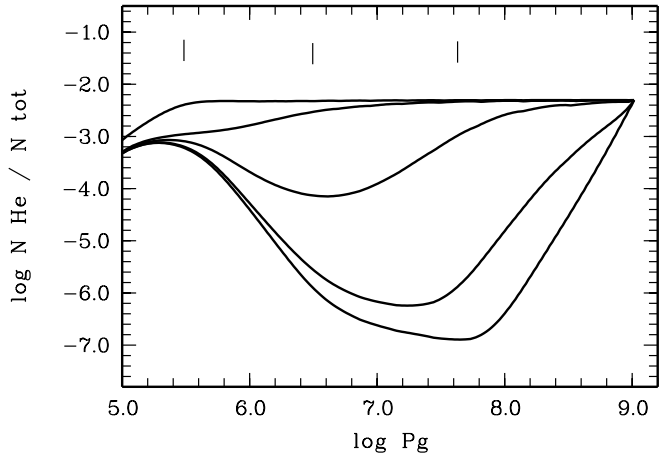

Fig. 1. Results of the diffusion calculations for a hydrogen rich white dwarf with $T_{\rm eff} = 80000$K, $\log g = 7.0$ and a solar helium abundance at the start. The number fraction of helium is plotted as a function of the gas pressure (in SI units) after (from top to the bottom) 10, 100, 1000, 5000 and 10000 y. In the upper part of the figure the Rosseland mean optical depths $\overline{\tau} = 1, 10, 100$, respectively, are indicated for the case after 10000 y

transitions the Lyman, Balmer and Paschen series are taken into account, for hydrogen the Lyman series only. The total radiative force due to each series is computed by numerical integration from the absorption edge to some maximal wavelength (e.g. 400Å for the Lyman series of He^+) with about 500 frequency points. The effect of line blends between the various lines of a series, which tends to reduce the radiative force, has been taken into account. For neutral helium the computation of the radiative force is similar as in Paper I with line broadening parameters of Dimitrijevic & Sahal-Bréchot (1984).

3. Results of the diffusion calculations

Fig. 1 illustrates the diffusion calculations for $T_{\rm eff} = 80000$K and $\log g = 7.0$. At time $t = 0$ in all depths He/H=0.005 and number fractions of the CNO elements of 0.0005 have been assumed. At the lower boundary at $P_{\rm g} = 10^9$Pa the composition remains the original one during the calculations. The gas pressure is related to the surface mass fraction q approximately by

$$q \approx \frac{4\pi G}{g^2} P_{\rm g} \tag{4}$$

So the mass of the layer considered is about $10^{-10} M_*$. 1000y after the onset of diffusion, the number fraction of helium near $\overline{\tau} = \frac{2}{3}$ is about 10^{-3} and does not decrease significantly during the following time, due to an equilibrium state between gravitational settling and radiative levitation is reached in the outer regions. In deeper layers, however, the separation of elements continues.

In Table 1 the results of the diffusion calculations at $\overline{\tau} = \frac{2}{3}$ are given for several effective temperatures and gravities. For

Table 1. From the diffusion calculations predicted logarithmic number fractions of elements at a Rosseland mean optical depth $\overline{\tau} = \frac{2}{3}$

$T_{\rm eff}$	$\log g$	He	C	N	O
100000	6.0	-2.2	-2.6	-2.5	-2.9
80000	6.0	-2.5	-3.3	-2.8	-3.5
60000	6.0	-3.5	-4.2	-3.8	-3.6
40000	6.0	-5.4	-4.5	-4.6	-5.3
100000	7.0	-3.1	-3.5	-3.6	-3.9
80000	7.0	-3.1	-4.1	-4.0	-4.2
60000	7.0	-4.2	-5.1	-4.8	-4.3
40000	7.0	-6.1	-5.4	-5.5	-6.3
100000	8.0	-5.7	-5.6	-4.4	-4.7
80000	8.0	-4.8	-5.4	-5.0	-4.7
60000	8.0	-5.1	-5.9	-5.8	-4.9
40000	8.0	< -7.1	-6.4	-6.6	-8.0

cases with $\log g = 6.0$ a time of 10000y has usually been necessary until the outer regions are near a diffusive equilibrium state. For cases with $\log g = 7.0$ time integrations over 1000y and 100y for $\log g = 8.0$ have been sufficient. To avoid numerical problems the initial abundances of helium and the heavy elements at $t = 0$ have been chosen somewhat larger than the expected ones, so that the elements sink during the diffusion calculations. For high effective temperatures and lower gravities the numerical code works sufficiently well, whereas the calculations are extremely time consuming in cases with lower $T_{\rm eff}$ and high gravities. The helium abundance for $T_{\rm eff} = 40000$K, $\log g = 8.0$ is an upper limit, because in this case we integrated over a time scale of four years only. Nevertheless the helium number fraction decreases by two orders of magnitude from an initial abundance of 10^{-5}. The elements C and N tend to be more abundant than helium. This is in favour of the result that heavy elements are responsible for the flux deficiency in the soft X-ray and EUV wavelength range of many DA white dwarfs with $T_{\rm eff} > 40000$K (Barstow et al. (1997) and references therein). In white dwarfs with $T_{\rm eff} > 60000$K or in those with $T_{\rm eff} \approx 60000$K and surface gravities $\log g < 8.0$, however, detectable amounts of helium should be present according to the diffusion calculations.

The results do not differ significantly from those of Vennes et al. (1988). Compared to observational results, the predictions for helium are too low by at least a factor of ten in the case of DAO stars (typically $T_{\rm eff} = 60000$K, $\log g = 7.0$ or somewhat larger) and central stars of planetary nebulae ($T_{\rm eff} = 100000$K, $\log g = 6.0$). For sdOB type stars ($T_{\rm eff} = 40000$K, $\log g = 6.0$) they are too low by more than a factor of 100 and cannot reproduce the typical abundance anomalies observed with deficiencies of carbon and solar abundances of nitrogen (Lamontagne et al., 1987).

With the data given in Table 2 the results for $T_{\rm eff} = 80000$K, $\log g = 7.0$ at $\overline{\tau} = \frac{2}{3}$ will be considered in detail. Helium is preferably doubly ionized. All ionization states have been taken into account in the calculations, the effect of neutral helium on the momentum balance is, however, negligibly small.

Table 2. Data at $\overline{\tau} = \frac{2}{3}$ for $T_{\rm eff} = 80000$K, $\log g = 7.0$. The gas pressure at this depth is $P_{\rm g} = 225000$Pa, the temperature $T = 80000$K, the chemical composition as given in Table 1. In the left part of the table is given the momentum per unit volume and unit time transferred on helium by gravitation, radiation (bound-bound and bound-free transitions), the electric field, partial pressure gradients, $\mathrm{He}^{++} - \mathrm{H}^{+}$ and $\mathrm{He}^{+} - \mathrm{H}^{+}$ collisions, respectively. The right part of the table shows the density of particles (in m^{-3}) in the ionization states of hydrogen and helium

momentum tansfer (SI units)	ionization (SI)
$n_{\rm He(tot)} m_{\rm He} g = -0.0498$	$n_{\rm H} = 5.6 * 10^{20}$
$n_{\rm He+} F_{\rm He+,rad,L} = 0.0092$	$n_{\rm H+} = 1.0 * 10^{23}$
$n_{\rm He+} F_{\rm He+,rad,C} = 0.0237$	$n_{\rm He} = 1.9 * 10^{15}$
$(n_{\rm He+} + 2n_{\rm He++})\, eE = 0.0127$	$n_{\rm He+} = 1.5 * 10^{18}$
$\frac{dp_{\rm He}}{dz} + \frac{dp_{\rm He+}}{dz} + \frac{dp_{\rm He++}}{dz} = 0.0041$	$n_{\rm He++} = 7.3 * 10^{19}$
$K_{\rm H+,He++}\,(w_{\rm H+} - w_{\rm He++}) = 8.7 * 10^{-5}$	
$K_{\rm H+,He+}\,(w_{\rm H+} - w_{\rm He+}) = -1.3 * 10^{-6}$	

The momentum per unit volume and unit time transferred to helium by gravity must be compensated by the momentum transferred by photons due to bound-bound and bound-free transitions, by the electric field, the gradient of the partial pressure and the momentum transfer due to collisions with all species of particles taken into account. For this example it can be seen that the radiative force $F_{\rm He+,rad,C}$ due to bound-free transitions exceeds the radiative force due to lines $F_{\rm He+,rad,L}$ by about a factor of 2.6. For larger gravities and lower effective temperatures helium sinks until the lines become desaturated and thus the bound-bound transitions become more important. For $T_{\rm eff} = 80000$K and $\log g = 8.0$ both contributions are approximately equal, for $T_{\rm eff} = 40000$K and $\log g = 8.0$ $F_{\rm He+,rad,L}$ exceeds $F_{\rm He+,rad,C}$ by a factor of 15 (the contribution of neutral helium is still small even for $T_{\rm eff} = 40000$K). If the contribution of the electrons to the line broadening would be neglected, this would lead to a momentum transfer by bound-bound transitions of 0.0083 instead of the value 0.0092 given in Table 2, which was obtained with the assumption of a quasistatic line broadening due to ions and electrons. Therefore uncertainties in line broadening theory are not of crucial importance, at least in this case. The momentum exchange due to collisions between helium and protons is small compared to the other contributions to the momentum equation. This indicates that for the given plasma conditions the ionization effects are negligible.

Fig. 2 shows the transformation of a helium-rich white dwarf with $T_{\rm eff} = 80000$K, $\log g = 7.0$ into a hydrogen-rich one by diffusion. An original number ratio $\mathrm{H/He} = 10^{-4}$ has been assumed in an outer layer of about $10^{-7} M_*$, the heavy elements have been neglected. After 1000 y the white dwarf is still helium rich, after 10000 y there is $\mathrm{H/He} = 1$ at $P_{\rm g} = 2.5 * 10^5$ or $\overline{\tau} = 0.9$, respectively. According to Eq. (4) this corresponds to a hydrogen layer mass of about $2 * 10^{-14} M_*$. After 100000 y the mass of the hydrogen layer would be about $7 * 10^{-13} M_*$, after 200000 y the mass would be $4 * 10^{-12} M_*$. For the latter case, the helium number fraction in the outer regions with $\overline{\tau} < 10$ is below 10^{-3}. So we conclude that, if the hydrogen number ratio in a DO white dwarf is 10^{-4} or larger, in the absence of mass loss it would transform into a DAO with an ultrathin hydrogen layer in not more than 10000 y. After 100000 y the surface composition would be very similar to the one predicted by the diffusion calculations for a thick hydrogen layer (see Table 1).

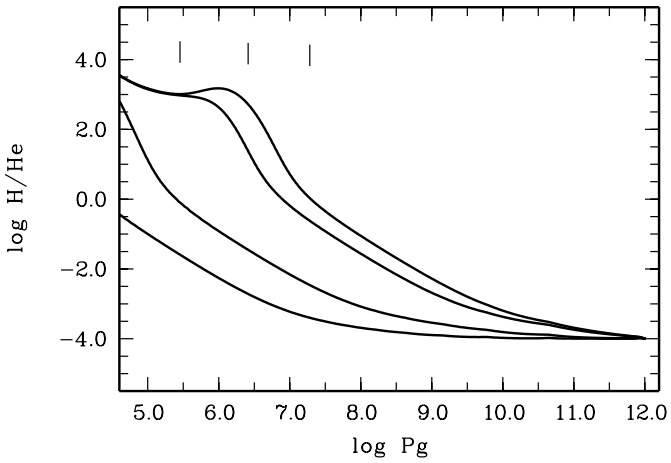

Fig. 2. Transformation of a helium-rich white dwarf with $T_{\rm eff} = 80000$K, $\log g = 7.0$ into a hydrogen-rich one by diffusion. The number fraction H/He is plotted as a function of the gas pressure (in SI units) after (from top to the bottom) 200000, 100000, 10000 and 1000 y. In the upper part of the figure the Rosseland mean optical depths $\overline{\tau} = 1, 10, 100$, respectively, are indicated for the case after 100000 y

4. The influence of mass loss

The diffusion velocitiy w_s is the mean velocity of the particles of species s in the center of mass system. In the presence of a wind there is a net mass flow, which is added to the diffusion flow:

$$j_s = n_s w_s + n_s v \tag{5}$$

The wind velocity v at each depth is obtained from the equation of continuity with the assumption of a depth-independent stellar radius R_*:

$$v = \frac{\dot{M}}{4\pi R_*^2} \frac{1}{\rho} \tag{6}$$

A stellar mass $M_* = 0.6 M_\odot$ is usually assumed (with one exception for subdwarfs).

For the calculations with mass loss the numerical method described in Paper II had to be slightly modified. Let j be the total flow (diffusion + wind) of a special species of particles and z the depth variable. We write for the gradient at a grid point i:

$$\frac{dj}{dz}\,(i) = \frac{j_{i+1/2} - j_{i-1/2}}{z_{i+1/2} - z_{i-1/2}} \tag{7}$$

For convenience, we use a half-mesh point notation here (in Paper II we denoted the half-mesh points with ib). The points i represent the zone centers, the points $i+1/2$ and $i-1/2$ denote the inner and outer boundaries, respectively. This equation is equivalent to Eq. (11) of Paper II. This evaluation of the flux at the half-mesh points corresponds to the control volume method

described by Hawley et al. (1984) and works sufficiently well for pure diffusion calculations. It is unstable, however, in cases with larger mass loss rates, where in the outer regions the wind velocity v exceeds the diffusion velocity w by several orders of magnitude. This instability is cured by evaluating the wind flow not at the zone boundary, but at the next grid point upstream or upwind. For example, if n is the density of the species of particles under consideration, we write for the flow at the zone boundary $i-1/2$:

$$j_{i-1/2} = n_{i-1/2} w_{i-1/2} + n_i v_i \tag{8}$$

This means, the diffusion part is treated according to the control volume approach, whereas for the wind part a modified upwind scheme is used. In the usual upwind scheme described by Hawley et al. (1984), the density only is evaluated at the next point upwind. Our method is more appropriate to satisfy the demand of mass conservation in each zone. Compared to the control volume method, the upwind scheme leads to some loss of accuracy, because the derivative of the flow is not centered at the point i. For $T_{\rm eff} = 80000$K, $\log g = 7.0$ and $\dot{M} = 10^{-14} M_*/y$ the mass loss rate is still small enough, so that both schemes could be used. The differences are not significant (less than 1%). In addition, for cases with larger mass loss rates a comparison with results obtained with a monotonic transport scheme, which can be considered as an improved upwind scheme with somewhat higher accuracy, did not lead to significant differences (about 3%).

The time steps are such that during one step the composition (e.g. the ratio $n_{\rm H}/n_{\rm He}$) does not change by more than 2%. The drawback of the numerical method is, that during many time steps at the outer grid points the composition oscillates around some mean value, which changes only slowly. One measure to reduce the computational effort is to update such quantities like opacities, radiative forces per particle and resistance coefficients only if the composition at one of the grid points has changed by at least 10%. Only the composition, the ionization equilibrium and the diffusion velocities must be updated after each time step. A second measure is to increase the distance between the grid points, especially in the outer regions. This allows larger time steps. With the gas pressure as independent variable we have used a grid spacing according to:

$$P_{\rm g}\,(i+1) = P_{\rm g}\,(i) + 0.1 * P_{\rm g}\,(i) + q \tag{9}$$

So from one grid point to another the gas pressure changes by 10% plus an additional constant q. For example, for $T_{\rm eff} = 80000$K, $\log g = 7.0$ and $\dot{M} \approx 10^{-13} {\rm M}_*/{\rm y}$ at the outer boundary $P_{\rm g}\,(0) = 40000{\rm Pa}$ is used and $q = 20000$. So especially the zones in the outer regions are expanded, the inner regions are less affected. This is justified, because in the outer regions is $v \gg w$, so that no significant concentration gradients occur. For this example, the regions with $P_{\rm g} < 10^6{\rm Pa}$ are lost within about one year. Within this time, the changes of composition due to diffusion are negligibly small. In spite of all this, the computations are still so time consuming that we can take into account the CNO elements in a few of the mass loss calculations only.

Table 3. Results for $T_{\rm eff} = 100000$K, $\log g = 6.0$ at $\overline{\tau} = \frac{2}{3}$ 10000 y after the onset of mass loss. The original number fraction of each element is 0.0714

$\dot{M}/\frac{y}{M_*}$	He	C	N	O
10^{-15}	0.0121	0.0074	0.0227	0.0516
10^{-14}	0.0329	0.0325	0.0332	0.0392

4.1. Cases with $\log g = 6.0$

For lower surface gravities the numerical code works sufficiently well, so that for some of the calculations the CNO elements can be taken into account. We first consider the case $T_{\rm eff} = 100000$K, typical for hot central stars of planetary nebulae. At $t = 0$ a composition He/H = C/H = N/H = O/H = 0.1 has been assumed. In Table 3 is given the predicted surface composition 10000 y after the onset of mass loss. For a mass loss rate of $10^{-15} M_*/{\rm y}$ the number fraction of helium decreases by a factor of 6 instead of a factor of ten in the diffusion calculations. Abundance anomalies of the heavy elements are predicted with a deficiency of carbon in comparison to oxygen and nitrogen. For $\dot{M} = 10^{-14} M_*/{\rm y}$ the number fraction of all elements decreases by about a factor of two only within 10000 y. Stronger winds prevent the elements from sinking. According to the review of Perinotto(1993) and the calculations of Pauldrach et al. (1988) typical mass loss rates for hot CSPN are of the order $10^{-9} M_*/{\rm y}$. Therefore we expect the effect of diffusion to be negligible.

Now we investigate the influence of mass loss for $T_{\rm eff} = 40000$K, $\log g = 6.0$. These stellar parameters are typical for subdwarfs near the hot end of the extended horizontal branch (EHB). Model atmosphere analysis of subdwarfs of typ sdOB or sdB yields underabundances of helium between a factor of two and 150 (e.g. Heber et al. (1984), Heber (1986), Moehler et al. (1990), Saffer et al. (1994)). In contrast to horizontal branch stars, the contribution of hydrogen burning to the total luminosity is negligible for EHB stars. This is because of the low mass of the hydrogen shell surrounding the helium burning core, which varies between $10^{-2} M_*$ for the sdB stars and 10^{-3} to $10^{-4} M_*$ for the sdOB stars near the helium main sequence. The subdwarfs stay near the EHB with almost unchanged stellar parameters for about $10^8{\rm y}$ (Caloi, 1989; Dorman et al., 1993). The helium abundances predicted from the diffusion calculations are clearly too low, in the absence of competing mechanisms helium sinks within 10000 y. Fig. 3 shows the results 40000 y after the onset of mass loss for a weak wind with $\dot{M} = 10^{-15} M_*/{\rm y}$. At $t = 0$ a solar composition has been assumed. The results differ drastically from those of the diffusion calculations without mass loss. Near $\overline{\tau} = \frac{2}{3}$ helium is now depleted by a factor of ten only, nitrogen has about the solar abundance and carbon is underabundant. A similar result has already been obtained by Michaud et al. (1985) and corresponds to the observed abundance anomalies. The problem, however, is the length of the time scales of stellar evolution. Therefore we have done some additional calculations for various mass loss rates over $10^8{\rm y}$. The results are summarized in Fig. 4. To save computation time

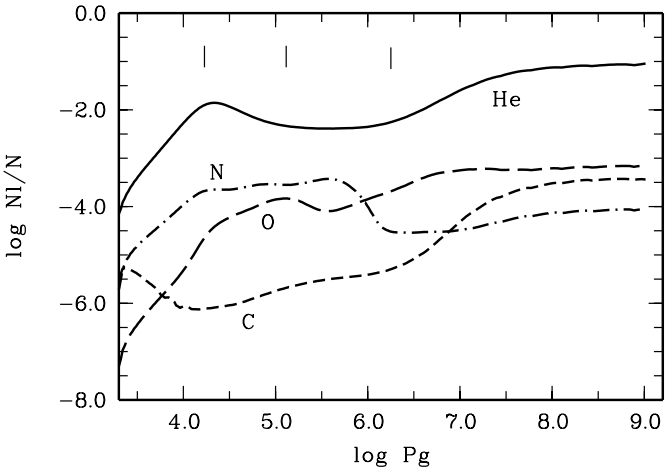

Fig. 3. Number fractions of He, C, N and O as a function of the gas pressure (SI units) for $T_{\rm eff} = 40000$K, $\log g = 6.0$, 40000 y after the onset of mass loss with $\dot{M} = 10^{-15} M_*/\mathrm{y}$. The optical depths $\overline{\tau} = 1, 10$ and 100 are indicated in the upper part of the figure

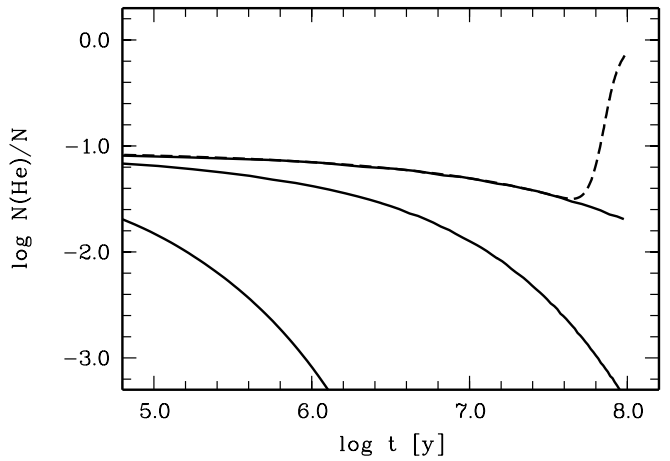

Fig. 4. Surface helium number fraction as a function of time for $T_{\rm eff} = 40000$K, $\log g = 6.0$ for (from top to the bottom) $\dot{M} = 5 * 10^{-13}, 10^{-13}$ and $10^{-14} M_*/\mathrm{y}$. The dashed line corresponds to $\dot{M} = 5 * 10^{-13}$ and $\mathrm{He/H} = 10^2$ instead of 0.1 at the lower boundary

the heavy elements and the ionization effects have been neglected. The lower boundary has been taken at $P_{\rm g} = 10^{12}$Pa, which corresponds to a mass depth of about $10^{-4} M_*$. At $t = 0$ a solar helium abundance has been assumed. The results show that a mass loss rate larger than 10^{-13} is required to account for the observed abundances. For $\dot{M} = 5 * 10^{-13} M_*/\mathrm{y}$ the surface helium abundance reduces to 0.05 after 10^7y and 0.02 after 10^8y. These values are typical for sdOB stars. To investigate the influence of the lower boundary condition on the surface abundance, we have done one calculation with a discontinuity in composition at the lower boundary (dashed line in Fig. 4). Instead of solar composition $\mathrm{H/He} = 10^{-2}$ is assumed at the lower boundary. For $\dot{M} = 5 * 10^{-13} M_*/\mathrm{y}$ the surface number fraction of helium reaches a minimum value of about 0.03 after $5 * 10^7$y, just as in the previous case. Then, however, it increases again. After 10^8y the star is transformed into a helium-rich sdO,

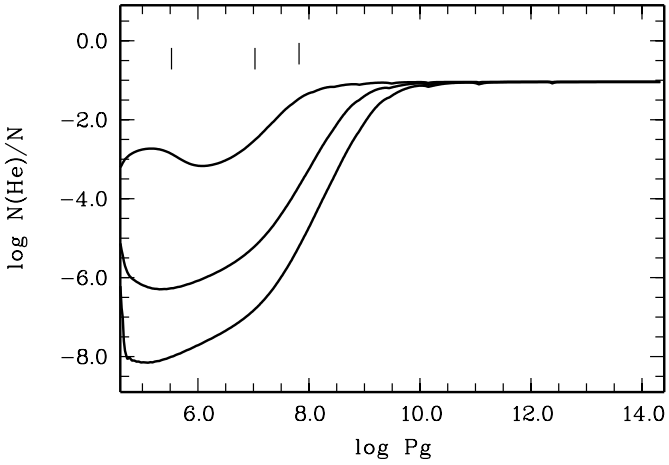

Fig. 5. Number fraction of helium as a function of the gas pressure (SI units) for $T_{\rm eff} = 80000$K, $\log g = 7.0$, $\dot{M} = 10^{-15} M_*/\mathrm{y}$ after 1000, 5000 and 10000 y (from top to the bottom). In the upper part of the figure the optical depths $\overline{\tau} = 1, 10$ and 100 are indicated for the case after 10000 y

for which $\mathrm{H/He} \approx 1$ is a typical value (Dreizler et al., 1990; Thejll et al., 1994).

4.2. DAO white dwarfs

In this section we investigate the time dependence of the helium abundance in the outer regions with a surface layer mass of about $10^{-5} M_*$ for a hydrogen rich white dwarf with $T_{\rm eff} = 80000$K and $\log g = 7.0$. In view of the numerical effort the CNO elements must be neglected to allow a time integration over 10^6y.

We now assume that the white dwarf has a thick hydrogen layer with a solar number fraction of helium. In Fig. 5 the results are shown for a weak wind with $\dot{M} = 10^{-15} M_*/\mathrm{y}$. After 10000 y only the outer regions are strongly depleted of helium with a number fraction of about 10^{-8}. In this case a weak wind would produce a DA white dwarf. Chayer et al. (1993, 1997) reported on a similar effect for heavy elements in the case of a weak wind. A mass loss rate of 10^{-14} is still too low. After 20000 y the helium abundance would reach a value similar as obtained in the diffusion calculations. In Fig. 6 we present the result for $\dot{M} = 2 * 10^{-13} M_*/\mathrm{y}$. The ionization effects have been neglected in these calculations. If they were taken into account, helium would sink somewhat more slowly. $\dot{M} = 1 * 10^{-13} M_*\mathrm{y}$ would then be sufficient to obtain nearly the same result. After $3 * 10^5$y the surface abundance is below the solar one by a factor of ten and is reduced by a factor of 50 after 10^6y. According to Blöcker (1995) and Vassiliadis & Wood (1994) these times are typical time scales of post AGB evolution, in which the star cools to $T_{\rm eff} = 80000$K and $T_{\rm eff} = 60000$K, respectively. This means that the diffusion time scales in the presence of mass loss with $\dot{M} \approx 10^{-13} M_*/\mathrm{y}$ are very similar to those of stellar evolution. The predicted surface abundances are larger than those predicted for the case of zero mass loss by a factor of 10 to 20. The surface abundances after 10^6y for several mass loss rates are

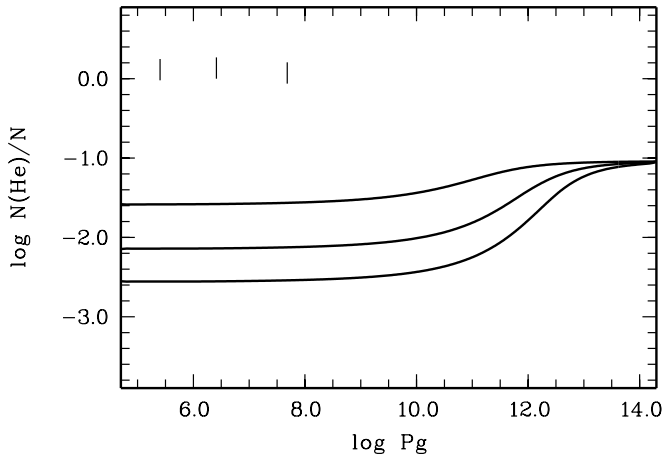

Fig. 6. The same as Fig. 5 for $\dot{M} = 2 * 10^{-13} M_*/\mathrm{y}$ and (from top to the bottom) 10^5, $5 * 10^5$ and 10^6y after the onset of mass loss and diffusion. $\overline{\tau} = 1, 10, 100$ is indicated for the case after 10^6y.

Table 4. Surface number fractions of helium for several mass loss rates in M_*/y for $T_{\mathrm{eff}} = 80000\mathrm{K}$, $\log g = 7.0$ after 10^6y

$\dot{M}$	$1 * 10^{-13}$	$2 * 10^{-13}$	$3 * 10^{-13}$	10^{-12}
n_{He}/n	0.0002	0.0028	0.0074	0.0332

given in Table 4. The results show, that for the cooler DAO's with helium abundances below the solar one, $\dot{M}$ should be in the range between 10^{-13} and $10^{-12} M_*/\mathrm{y}$. The calculations have shown, that these results do not differ by more than about a factor of two, if $T_{\mathrm{eff}} = 60000\mathrm{K}$ instead of $T_{\mathrm{eff}} = 80000\mathrm{K}$ is assumed.

From the results an explanation of the helium abundances in DAO white dwarfs with mass loss and a thick helium layer seems to be possible. However, other possible explanations, e.g. a less massive hydrogen layer and a weaker wind cannot be excluded as long as the mass loss rate is not known independently. The calculations of stellar evolution predict hydrogen layer masses between 10^{-5} and $10^{-4} M_*$, which however, may vary from star to star (Blöcker et al., 1997).

4.3. The transformation from DO's into DA's

In Fig. 2 of Sect. 3 we investigated the transformation of a helium-rich DO white dwarf into a DAO in the absence of mass loss for an initial hydrogen number fraction of 10^{-4}. Curve 1 in Fig. 7 shows the H/He abundance profile after 50000 y. A thin hydrogen layer with a mass of about $10^{-13} M_*$ floats ontop of the helium rich regions. According to Bergeron et al. (1994) this is an upper limit for the mass of the hydrogen layer if the helium abundances of DAO stars were to be explained with stratified atmospheres, in most cases it must even be less massive by a factor of 10 to 100. Now we ask, what would happen with a white dwarf with a stratified atmosphere in the presence of mass loss. Curves 2 and 3 in Fig. 7 show the abundance profiles 1000 and 5000 y, respectively, after the onset of a weak wind with $\dot{M} = 10^{-16} M_*/\mathrm{y}$. Within 5000 y the DAO white dwarf would

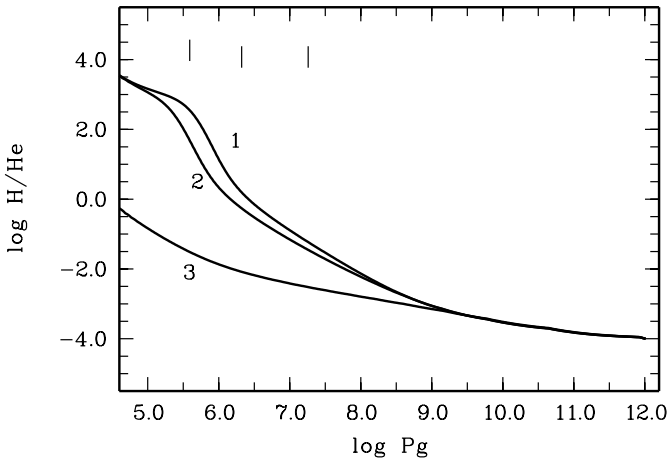

Fig. 7. The influence of mass loss on a stratified H/He layer for $\dot{M} = 10^{-16} M_*/\mathrm{y}$ and $T_{\mathrm{eff}} = 80000\mathrm{K}$ and $\log g = 7.0$. Curve 1 is the result of diffusion calculations after $50000\mathrm{y}$ for an original composition $\mathrm{H/He} = 10^{-4}$. Curves 2 and 3 show the composition 1000 and $5000\mathrm{y}$, respectively, after the onset of mass loss. In the upper part of the figure $\overline{\tau} = 1, 10$ and 100 is indicated for the case after $1000\mathrm{y}$

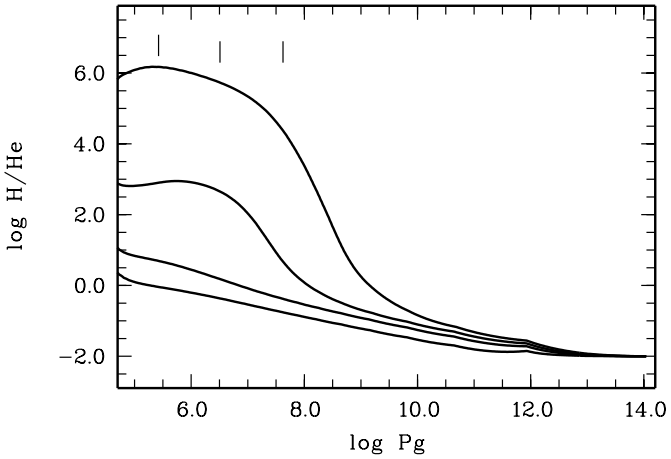

Fig. 8. Transformation of a DO white dwarf with $\mathrm{H/He} = 10^{-2}$ by number and $T_{\mathrm{eff}} = 80000\mathrm{K}$, $\log g = 7.0$ in the presence of mass loss with $\dot{M} = 2 * 10^{-15} M_*/\mathrm{y}$. The composition is plotted as a function of the gas pressure (in SI units) for (from top to the bottom) 400000, 250000, 150000 and $50000\mathrm{y}$ after the onset of mass loss. The optical depths $\overline{\tau} = 1, 10$ and 100 are indicated for the case after $250000\mathrm{y}$

tranform back into a DO. This means that DO's with a hydrogen number fractions of 10^{-4} or lower will not transform into DAO's or DA's if at least a weak wind is present. However, the hypothesis, that DAO's have thin hydrogen layers and are the descendants of former DO's cannot be excluded, because there are too many unknowns, the mass loss rate and the hydrogen number fraction in DO's. Under certain conditions a floating up scenario may be possible, as shown in Fig. 8. We start from a DO with a hydrogen number fraction of 10^{-2} and assume a mass loss rate of $\dot{M} = 2 * 10^{-15}/\mathrm{y}$. After 50000 y it would be tranformed into a hybrid star with $\mathrm{H/He} \approx 1$ in the outer regions. After 150000 y the surface abundance would approximately the solar one. After 250000 y we obtain $\mathrm{H/He} \approx 10^{-3}$

and the star would appear as a DAO white dwarf. As for $\overline{\tau} < 5$ the composition is constant within 10%, the atmosphere would appear to be chemically homogenous, although the outer layers are stratified. Finally, after 400000 y the helium abundance sinks below 10^{-6} and the star is a DA. These time scales are extended, if the mass loss rate is somewhat larger. For example, for $\dot{M} = 10^{-14} M_*/\mathrm{y}$ the DO would transform into a hybrid white dwarf with 30 % hydrogen and 70 % helium after 100000 y. A mass loss rate of $\dot{M} = 10^{-13} M_*/\mathrm{y}$, however, would prevent the transformation. In this case a white dwarf with a hydrogen layer mass of $10^{-10} M_*$ would be retransformed into a helium-rich one within some thousands of years. A similar result has already been obtained by Michaud (1987).

We conclude that stratified atmospheres with an abundance profile derived from an equilibrium between gravitational settling and ordinary diffusion cannot exist, if at least a weak wind of $10^{-16} M_*/\mathrm{y}$ is present. DO's with hydrogen number fractions of 10^{-2} or less do not transform into DA's, if the mass loss rate is larger than about $10^{-13} M_*/\mathrm{y}$.

5. Discussion

According to the diffusion calculations, for $\log g = 7.0$ the surface number fraction of helium reaches a maximum value of about 10^{-3} near $T_{\mathrm{eff}} = 80000\mathrm{K}$. The momentum transferred on helium by bound-free transitions is essential for these stellar parameters, whereas the ionization effects and the exact shape of the He^+ line profiles turned out to be of minor importance. For $T_{\mathrm{eff}} = 60000\mathrm{K}$ the predicted number fraction is below 10^{-4}, which is lower by at least a factor of ten than observed in DAO white dwarfs (Bergeron et al., 1994, Napiwotzki, 1995). According to Chayer et al. (1995) the simplified treatment of the radiative transfer (use of the diffusion approximation as described Papers I and II) gives quite reasonable estimates of the surface abundance of levitating elements. So we expect that a model atmosphere approach would not change the situation significantly.

The failure of the diffusion calculations is not surprising, because the results of Sect. 4 have shown that the helium abundances in hot white dwarfs cannot be understood without the effect of mass loss, which , compared to the diffusion calculations, may lead to over- or underabundances of helium by several orders of magnitude. Recently, Werner et al. (1995) and Dreizler et al. (1995) detected in the spectra of five DO and one DAO white dwarf metal absorption lines of ultrahigh ionization states, which are possibly due to a stellar wind. However, the mass loss rates are not known. To discuss the results we will use a formula from Blöcker (1995), which is based on theoretical mass loss rates for central stars of planetary nebulae (Pauldrach et al., 1988).

$$\dot{M} = 1.29 * 10^{-15} L^{1.86} \qquad (10)$$

L is the stellar luminosity in solar units and $\dot{M}$ is the mass loss rate in $M_\odot/\mathrm{y}$. We use this equation to extrapolate the mass loss rates into the region of white dwarfs and subdwarfs. To account for the observed helium abundaces in sdOB stars, we inferred in Sect. 4.1 for $T_{\mathrm{eff}} = 40000\mathrm{K}$, $\log g = 6.0$ a mass loss rate of $5 * 10^{-13} M_*\mathrm{y}$, which is necessary to prevent helium from sinking too rapidly. For a typical subdwarf mass of $0.5 M_*$ Eq. (10) yields $\dot{M} \approx 10^{-12} M_*/\mathrm{y}$. The theoretical formula of Abbott (1982) for radiatively driven hot star winds yields $\dot{M} = 5 * 10^{-12} M_*/y$ for a solar metallicity. However, it predicts a nearly linear decrease of $\dot{M}$ with decreasing metallicity. For hot main sequence stars Kudritzki et al. (1987) obtain a mass loss rate reduced by about a factor of three, if the metallicity is reduced by a factor of ten. As the metal abundances in white dwarfs and subdwarfs are different from the solar one, the values for $\dot{M}$ used in the discussion below are rough estimates only. In the following we will neglect the difference between solar and stellar masses for the mass loss rate.

MacDonald & Arrieta (1994) modelled the evolution of sdB's into sdO's in the presence of mass loss. They have shown that, at least for solar metallicity, the sdB's may loose most of their hydrogen envelope during their evolution into the sdO region in the HRD. Our results indicate, that for a mass loss rate necessary to prevent helium from sinking too rapidly, the transformation of helium-deficient subdwarfs into helium-rich ones is possible. These results favour the hypothesis of an evolutionary link between the sdB's and sdO's, which is expected from the evolutionary tracks of Dorman et al. (1993) and Caloi (1989). For clarification it would be necessary to incorporate mass loss and diffusion into the calculations of stellar evolution. When the star leaves the EHB, the luminosity and thus the mass loss rate tends to increase. This effect will accelerate the transformation into a helium rich one.

Koesterke et al. (1998) investigated the winds of PG 1159 stars with $T_{\mathrm{eff}} > 100000\mathrm{K}$ and $\log g \approx 6$. They derived mass loss rates which are of the order 10^{-7} to 10^{-8}. With the luminosities given by these authors, these order of magnitudes are in accordance with Eq. (10). The results of Sect. 4.1 have shown that for $\dot{M} = 10^{-14}$ the surface composition would change by a factor of two only within $10^4\mathrm{y}$. Therefore the effect of diffusion on the surface composition seems to be neglibible small in these stars. This is the probable reason why the diffusion calculations presented in Papers I and II cannot explain the observed abundances. As the influence of diffusion near the stellar surface decreases with increasing mass loss rate, it should be negligible in central stars of planetary nebulae and hot PG 1159 stars.

For $\log g = 7.0$ and T_{eff} between $80000\mathrm{K}$ and $60000\mathrm{K}$ the expected mass loss rates according to Eq. (10) are of the order 10^{-12} to 10^{-13}. For these rates the effect of diffusion is not negligible. Therefore, on the one hand the surface abundance of helium will be lower than the solar one. On the other hand helium sinks so slowly, that the surface abundance after $\approx 10^6\mathrm{y}$ is still larger than predicted by the diffusion calculations. Therefore the presence of helium in DAO white dwarfs can be explained with the assumptions of a thick hydrogen layer and mass loss rates in this range. If the mass loss rate is below a critical value, we expect a strong depletion of helium. Therefore in the $\log g$ - T_{eff} diagram a line should exist, which separates the DAO's from the DA's, as indicated in Fig. 9. The line has been obtained from the condition that for all stars below this

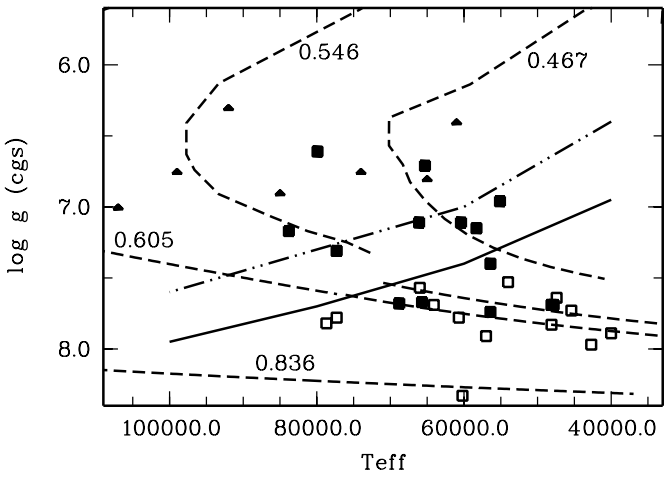

Fig. 9. Predicted separation line between the DAO's and DA's in the $\log g$ - $T_{\rm eff}$ diagram for $\dot{M}$ according to Eq. (10) and for mass loss rates reduced by a factor of ten (dashed-dotted line). The DAO's analyzed by Napiwotzki (1995) are marked (filled triangles) as well as the DAO's (filled squares) and the DA's (open squares) analyzed by Bergeron et al. (1994). The dashed lines indicate a post-EHB track from Dorman et al. (1993) with $M_* = 0.467 M_\odot$ and post AGB-tracks from Schönberner (1983), Koester & Schönberner (1986) and Blöcker (1995), respectively

.

line the surface helium number fraction decreases below 10^{-3} within 10^5y. The mass loss rates given by Eq. (10) have been assumed. In all white dwarfs and subdwarfs above this line helium should be present, if the time scales of stellar evolution are not much larger than 10^5y. If the cooling were taken into account, especially for lower values of $T_{\rm eff}$ we expect the line to be shifted to somewhat lower gravities, because for these stars the cooling ages are significantly larger than 10^5y. All single white dwarfs with thick hydrogen layers below the line should be DA's, their helium abundances may be lower than predicted by the diffusion calculations. Bergeron et al. (1994) detected some DAO's, which are clearly in the DA region. These authors suggest that some of them are members of possibly interacting binary systems. The others should be in a DO/DA transition state. Napiwotzki (1995) analyzed some extremely hot objects without detectable helium lines, which are above the separation line. However, as helium is more difficult to detect in the spectra of very hot stars, the upper limits on the helium number fraction are between the solar one and about 10^{-2}. Therefore these results do not rule out the mass loss hypothesis, which hardly could explain the absence of helium in these objects. For almost all hot DA's analyzed by Finley et al. (1997), our results predict the absence of helium, if they have a thick hydrogen layer.

If the mass loss rates are smaller by a factor of ten than obtained from Eq. (10), the separation line would be shifted by about 0.4 dex to lower gravities, as indicated by the dashed-dotted line in Fig. 9. In this case, the presence of helium especially in the hotter and lower gravity DAO's analyzed by Napiwotzki (1995) can still be explained with mass loss, whereas most of the cooler ones analyzed by Bergeron et al. (1994) should be DA's, if they have a thick hydrogen layer. The comparison of the position of the DAO's in the $T_{\rm eff}$ - $\log g$ diagram with theoretical evolutionary tracks indicates, that many of the cooler DAO's are post-EHB stars, as suggested by Bergeron et al. (1994). As discussed above, the hydrogen-rich sdB's or sdOB's, respectively, probably evolve into helium rich sdO's. During the cooling, hydrogen will float up and transform them into DAO's. Therefore the outer regions of these objects are possibly stratified. As the H/He abundance profile is smeared out in the presence of mass loss, the atmospheres may appear to be chemically homogenous.

If the DB gap is real, then all DO white dwarfs should be transformed into DA's until they have cooled down to 45000 K. In which stage of evolution the transformation occurs, depends on the mass loss rate and on the number fraction of hydrogen in the DO white dwarf. Dreizler & Werner (1996) note, that the relative number of DA to non-DA stars continuously increases from the hot end of the cooling sequence to the DB gap. The absence of mass loss would require $\rm H/He \ll 10^{-4}$ in hot DO's, because otherwise they would transform into DAO's already before they have cooled down to $T_{\rm eff} \approx 80000$K. A weak wind of $\dot{M} \approx 10^{-16}$ would be sufficient to prevent the transformation for $T_{\rm eff} = 80000$K, $\log g = 7.0$ and $\rm H/He = 10^{-4}$. For $\rm H/He = 10^{-2}$ and the same stellar parameters $\dot{M} \approx 10^{-13}$ would be required. We have done some additional calculations for $T_{\rm eff} = 60000$K. For $M_* = 0.6 M_\odot$, a surface gravity $\log g \approx 7.8$ and according to Eq. (10) $\dot{M} \approx 10^{-14}$ is expected. A DO with $\rm H/He = 10^{-3}$ would still be helium rich after some 10^5y, whereas a DO with $\rm H/He = 10^{-2}$ would transform into a DA. So we conclude that the DO's which transform into DA's before they have cooled down to 60000K should have $\rm H/He > 10^{-3}$ when they enter the cooling sequence. The others will transform later. An example probably is HD 149499B with $T_{\rm eff} = 49500$K, $\log g = 8.0$ and $\rm logH/He = -0.65$ (Napiwotzki et al., 1995, 1996; Dreizler & Werner, 1996). In other DO white dwarfs with similar stellar parameters, however, Dreizler & Werner (1996) did not find any hydrogen. There should be a real chance to detect more hybrid white dwarfs or such with about solar helium abundances, because in the presence of mass loss this transition phase takes about 10^5y. The search for hydrogen in helium-rich pre-white dwarfs indicates that a variety of hydrogen abundances may occur. Dreizler et al. (1996) and Napiwotzki & Schönberner (1995) detected some hybrid objects, whereas for two other PG 1159 stars and one DO white dwarfs Werner (1996) gives an upper limit of 5% for the number fraction of hydrogen.

From the results an increase of the number ratio of DA's to non-DA's from the hot end of the cooling sequence to lower effective temperatures seems to be plausible. A continuous distribution of hydrogen abundances in stars at the hot end should lead to a continuous distribution of the time scales, in which hydrogen floats up. To clarify the question if the results can explain quantitatively the observed ratio of DA and non-DA stars and the hydrogen layer masses obtained by asteroseismology of the pulsating ZZ Ceti white dwarfs (see e.g. Bradley & Klein-

man, 1997) diffusion and mass loss and the cooling of the white dwarfs must be taken into account simultaneously.

Acknowledgements. We thank R. Napiwotzki for carefully reading the manuscript and useful comments

References

Abbott D.C., 1982, ApJ 259, 282
Babel J., Michaud G., 1991, A&A 248, 155
Barstow M.A., Holberg J.B., Hubeny I., Lanz T., 1997, in White Dwarfs, eds. J. Isern, M. Hernanz, E. Garcia-Berro, p237
Bergeron P., Wesemael F., Beauchamp A. et al., 1994, ApJ 432, 305
Blöcker T., 1995, A&A 299, 755
Blöcker T., Herwig F., Driebe T., Bramkamp H., Schönberner D., 1997, in White Dwarfs, eds. J. Isern et al., Kluwer Academic Publishers
Bradley P., Kleinman S., 1997, in White Dwarfs, eds. J. Isern, M. Hernanz, E. Garcia-Berro, p445
Burgers J.M., 1969, Flow Equations for Composite Gases, Academic Press, New York
Caloi V., 1989, A&A 221, 27
Chapman S., Cowling T.G., 1970, The Mathematical Theory of Non-Uniform Gases, 3rd ed., Cambridge University Press
Chayer P., Pelletier C., Fontaine G., Wesemael F., 1993, in White Dwarfs: Advances in Observation and Theory, ed. M.A. Barstow, Kluwer Academic Publishers
Chayer P., Vennes S., Pradhan A. et al., 1995, ApJ 454, 429
Chayer P., Fontaine G., Pelletier C., 1997, in White Dwarfs, eds. J. Isern, M. Hernanz, E. Garcia-Berro, Kluwer Academic Publishers, p253
Dimitrijevic M.S., Sahal-Brechot S., 1984, JQSRT 31, 301
Dorman B., Rood T.B., O'Connel R.O., 1993, ApJ 419, 596
Dreizler S., Werner K., 1996, A&A 314, 217
Dreizler S., Heber U., Werner K., Moehler S., de Boer K.S., 1990, A&A 235, 234
Dreizler S., Heber U., Napiwotzki R., Hagen H.J., 1995, A&A 303, L53
Dreizler S., Werner K., Heber U., Engels D., 1996, A&A 309, 820
Finley D.S., Koester D., Basri G., 1997, ApJ 488, 375
Fontaine G., Wesemael F., 1987, in IAU Coll. No. 95, The second conference on faint blue stars, eds. A.G.D. Phillip, D.S. Hayes & J. Liebert, Davis Press, p285
Fontaine G., Wesemael F., 1997, in White Dwarfs, eds. J. Isern, M. Hernanz, E. Garcia-Berro, Kluwer Academic Publishers, p173
Geiss J., Bürgi A., 1986, A&A 159, 1
Gonzales J.F., LeBlanc F., Artru M.C., Michaud G., 1995, A&A 297, 223
Hawley J.F., Smarr L.L., Wilson J.R., 1984, ApJS 55, 211
Heber U., 1986, A&A 155, 33
Heber U., 1992, in The Atmospheres of Early-Type Stars, U. Heber and C.S. Jeffery (eds.), Springer Verlag, p234
Heber U., Hunger K., Jonas G., Kudritzki R.P., 1984, A&A 130, 119
Hooper C.F. Jr., 1967, Phys. Rev. 165, 215
Hunter G., Kuriyan M., 1977, Proc. Roy. Soc. London A, 353, 575
Koesterke L., Dreizler S., Rauch T., 1998, A&A 330, 1041
Koester D., 1989, ApJ 342, 999
Koester D., Schönberner D., 1986, A&A 154, 125
Kudritzki R.P., Pauldrach A., Puls J., 1987, A&A 173, 293
Lamontagne R., Wesemael F., Fontaine G., 1987, ApJ 318, 844
MacDonald J., Arrieta S.S., 1994, in Proc. "Hot Stars in the Halo", eds. S.J. Adelman, A.R. Upgren, C.J. Adelman, Cambridge University Press, p238
Massacrier G., 1996, A&A 309, 979
Massacrier G., El-Murr K., 1996, A&A 312, L25
Michaud G., 1987, in IAU Coll. No. 95, The second conference on faint blue stars, eds. A.G.D. Phillip, D.S. Hayes & J. Liebert, Davis Press, p249
Michaud G., Martel A., Ratel A., 1978, ApJ 226, 483
Michaud G., Montmerle T., Cox A.N. et al., 1979, ApJ 234, 206
Michaud G., Bergeron P., Wesemael F., Fontaine G., 1985, ApJ 299, 741
Michaud G., Bergeron P., Heber U., Wesemael F., 1989, ApJ 338, 417
Mihalas D., 1978, Stellar Atmospheres, 2d ed.; San Francisco: Freeman
Moehler S., Heber U., de Boer K.S., 1990, A&A 239, 265
Napiwotzki R., 1995, in White Dwarfs, eds. D. Koester & K. Werner, Lecture Notes in Physics 443, Springer Verlag, p176
Napiwotzki R., Schönberner D., 1993, in White Dwarfs: Advances in Observation and Theory, ed. M.A. Barstow, NATO ASI Series Vol. 403
Napiwotzki R., Schönberner D., 1995, A&A 301, 545
Napiwotzki R., Hurwitz M., Jordan S. et al., 1995, A&A 300, L5
Napiwotzki R., Jordan S., Bowyer S. et al., 1996, in Astrophysics in the Extreme Ultraviolet, eds. S. Bowyer, R.F. Malina, Kluwer Academic Publishers, p241
Newman J.H., Cogan J.D., Ziegler D.L. et al., 1982, Phys. Rev. A, 25, 2976
Oxenius J., 1986, Kinetic Theory of Particles and Photons, Springer Verlag, Heidelberg, New York, Tokyo
Paquette C., Pelletier C., Fontaine G., Michaud G., 1986, ApJS 61, 177
Pauldrach A., Puls J., Kudritzki R.P., Mendez R.H., Heap S.R., 1988, A&A 207, 123
Perinotto M., 1993, IAU Symp. No. 55, eds. R. Weinberger & A. Acker, p57
Peterson D.M., Theys J.C., 1981, ApJ 244, 947
Radzig A.A., Smirnov B.M., 1985, Reference Data on Atoms, Molecules and Ions, Springer Verlag, Berlin
Saffer R.A., Liebert J., 1995, in White Dwarfs, eds. D. Koester & K. Werner, Lecture Notes in Physics 443, Springer Verlag, p221
Saffer R.A., Bergeron P., Koester D., Liebert J., 1994, ApJ 432, 351
Schönberner D., 1983, ApJ 272, 708
Shipman H.L., 1997, in White Dwarfs, eds. J. Isern, M. Hernanz, E. Garcia-Berro, Kluwer Academic Publishers, p165
Suchy K., 1984, in Encyclopedia of Physics, Vol. XLIX/7: Geophysics III, Part VII, p.57, Springer Verlag
Thejll P., Bauer F., Saffer R. et al., 1994, ApJ 433, 819
Underhill A.B., Waddell J.H., 1959, National Bureau of Standards Circular 603
Unglaub K., Bues I., 1996, A&A 306, 843 (Paper I)
Unglaub K., Bues I., 1997, A&A 321, 485 (Paper II)
Vassiliadis E., Wood P.R., 1994, ApJS 92, 125
Vennes S., 1992, ApJ 390, 590
Vennes S., Fontaine G., 1992, ApJ 401, 288
Vennes S., Pelletier C., Fontaine G., Wesemael F., 1988, ApJ 331, 876
Werner K., 1996, A&A 309, 861
Werner K., Dreizler S., Heber U. et al., 1995, A&A 293, L75